Chapter

Lead-Free Hybrid Perovskite Light-Harvesting Material for QD-LED Application

Rajan Kumar Singh, Neha Jain, Sudipta Som, Somrita Dutta, Jai Singh and Ranveer Kumar

Abstract

Most recently, organic-inorganic semiconductor light harvester materials, have arisen as a new class of functional element and attracts the research community due to its outstanding optoelectronic properties. Organic-inorganic perovskites are solution process that is easy for the fabrication of devices at low temperature. Additionally, up to date, perovskite quantum dots have emerged as the most efficient light harvester for LEDs and display applications, with high color purity, color tunability, and photoluminescence quantum yield up to 100%. However, the presence of lead in organic-inorganic perovskites and the stability issue of perovskite materials are the significant challenges for the research community. To date, some lead substitute materials have been tried to enhance the film morphology and production of the less toxic light harvester. In this chapter, we focus on the lead substitution on B sight with homovalent cations like Sn^{2+}, Mn^{2+}, Cd^{2+}, and Zn^{2+} cations. These lead substitutions not only reduce the toxicity of perovskite material while these dopants also enhance the optical and performance of LEDs. We also included the LEDs application of lead substituted perovskite quantum dots (PQDs) that may be useful for the environmental friendly and highly performing perovskite quantum dot LEDs (PQ-LEDs) shortly.

Keywords: hybrid perovskite, quantum dots, lead-free, light emitting diodes

1. Introduction

Organic-inorganic perovskite light harvesting materials have attracted passionate interest in past few years and raised as one of the most promising solar cells with power conversion efficiency up to 23% as well as excellent performance in LED display devices with high color gamut and color purity [1]. For the photovoltaic (PV) application, perovskite materials were first used in 2009 and for QDs LED applications, perovskite material was used firstly in 2014 [2]. Perovskite-based devices are solution processable that makes it cost-effective and helps in large scale production. Presently, such kind of perovskite solar cells is now comparable to the commercially available solar cells including, silicon, CdTe, CuInGaSe, and GaAs [3]. Perovskite quantum dots (PQDs) also are the most research centered topic in the field of nano-materials and colloidal QDs due to its excellent optical behavior as explained earlier [4].

After long research and development, semiconductor QDs (CdSe, CdZnSe, InP, etc.) and OLEDs have emerged as the leading technologies in the field of display devices [3]. OLEDs have lit pixels, less energy consuming properties, superior contrast, and wider viewing angles. However, synthesis and fabrication process of OLEDs are very complicated that raise the price of devices. On the other hand, PQDs possess tunable, narrow band emission and high PLQY that significantly improve the performance in both EL and PL devices as explained earlier. Existing CdSe and InP QDs have taken decades to be suitable as the robust candidates for displays. Samsung QLED TVs have been in the forefront serving the premium market along with Chinese brands, TCL and Hisense. Samsung Display is building a pilot production facility for QD OLED, which will start production in 2019. Most research is centered on PQDs due to their high photoluminescence (PLQY), tunable band gaps, and narrow emission wavelength. With quantum confinement effects, the emission of PQDs can be controlled with size and ingredients. Hence, PQDs are useful in photovoltaic cells, laser applications, light-emitting diodes (LEDs), and bio-imaging. Promising color purity and emission tunability of QDs make them promising contenders for next-generation displays as a light converter (white-light LEDs) and active-mode QD-LEDs (QLEDs) [3, 5]. Additionally, PQDs work faster than other QDs due to the absence of a deep state, where the electron-hole pair does not immediately revert to its ground state. In this context, PQDs have become promising candidates for the next-generation of w-LEDs for lighting and other display applications [6–9]. After the discovery of PQDs, more than 7000–8000 peer-reviewed literatures have been published. The fast rate of scientific research publication reveals the interest of the research community in the PQDs topic. Besides excellent performances of PQD technology, some challenges restrict the lead-containing perovskite materials for commercialization. Lead halide perovskite both bulk as well as nanoparticles/QDs are soft and very sensitive with humidity, moisture, light, air, temperature, etc. [10]. Therefore, the most apparent work necessity is to develop the new synthesis routes and new approaches of their more stabilization concerning ambient conditions, water, light, and temperature. Bromide-based perovskite has excellent performance, but the major shortcoming is the stability and presence of toxic element Pb. In this regards, a more in-depth understanding of the mechanism on the radiative and nonradiative recombination is necessarily required [11, 12].

Thus it is an open question that does the organic-inorganic perovskite-based device industry fabrication comes soon? The answer may be controversial because research community will say yes while some will say no because of the toxicity of Pb and long term stability of the materials. According to the U. S. EPA, the maximum amount of Pb^{2+} in air and water should not be more than 0.1 μg L^{-1} and 15 μg L^{-1} respectively [13]. Hence mass production of pure Pb-based perovskite may pollute the Earth due to its toxicity, long degradation lifetime and easy solubility in water. Therefore, we need to develop a new approach to explore environmental friendly Pb free or limited amount of Pb-based perovskite materials for optoelectronic applications. Thus these two main drawbacks of perovskite material restrict it in commercialization. Hence, the demand for nontoxic element-based perovskite materials continues to grow in the past few years [14]. Among these nontoxic alternatives, divalent tin cation has been considered as a right candidate in replacing Pb^{2+}, and the application of tin-halide perovskites in optoelectronic devices has also been investigated. However, Sn^{2+} undergoes facile oxidation to its tetravalent state (Sn^{4+}), creating a high defect density in the perovskite lattice. These defects would generate trap states in the middle of the band gap, leading to rapid non-radiative relaxation of the exciton. The highest PLQY value of tin-based perovskite nanomaterials can only reach 6.4%, which is still far inferior to the lead-based perovskite

nanomaterials (~84%) [15]. Potential applications of Sn-based perovskite material in optoelectronic applications, significant efforts have been made recently to improve the photoluminescence properties of tin perovskite-based nanomaterials. Besides Sn, in place of Pb^{2+}, Zn^{2+}, Mn^{2+}, Ge^{2+}, Cu^{2+}, and Bi^{3+} already have been investigated for less lead of lead-free perovskite materials for versatile applications. However, in the case of organic-inorganic halide PQDs, there is very less work reported and some research work based on Pb^{2+} substitution in only inorganic $CsPbX_3$ perovskite systems are going on, and this will be the main focus for the present chapter.

2. Structure of halide perovskite

Perovskites structure derives from the crystal structure of titanium calcium oxide ($CaTiO_3$). This was the first discovered perovskite material in the year 1839 by German mineralogist Gustav Rose and structure of perovskite material was studied by Russian mineralogist Lev A. Perovski [16]. After this discovery, a huge amount of perovskite materials have been found from natural resources and as well as synthesized in the lab also. So perovskite materials can be categorized mainly into two categories, one is based on oxides (oxygen anion) and another based on halides (halogen anions). On the basis of this categorization, perovskite materials adopt ABO_3 and ABX_3 chemical formula, where A and B are the cations and X is halogens such as I, Br, Cl, or mixed halides. ABO_3 structured perovskite is generally used for thermoelectric, superconductive and ferromagnetic applications which were discovered in the 18th century. On the other hand, halide-based perovskite material; $CsPbX_3$ was first reported in 1958, and $CH_3NH_3PbX_3$-based perovskite was seen in 1978. Thus ABX_3 perovskite further can be categorized into two subparts, pure inorganic halide perovskite, and organic-inorganic halide perovskite. Mitzi et al. have first time reported the excitonic property of halide perovskites for light-emitting diodes (LEDs) and thin film transistors in the year 1990 [17]. Nowadays, most extensively studied materials are ABX_3 structured perovskite semiconductor due to its excellent properties. In ABX_3 chemical formula, A, belongs to monovalent inorganic cation such as K^+, Rb^+, Cs^+ or monovalent organic cation like ethylammonium ($CH_3CH_2NH_3^+$, EA), methylammonium ($CH_3NH_3^+$, MA^+), formamidinium ($CH(NH_2)^{+2}$), FA), B-site stands for divalent cation Pb^{2+}, Sn^{2+}, Ge^{2+}, Ca^{2+}, Sr^{2+}, Ba^{2+} and X is anion (I^-, Br^- and Cl^-). The properties of perovskite material can be easily tuned by changing the A, B or X site in ABX_3 structure [18]. Generally, perovskite materials have cubic structure consists of close-packed AX_3 sub-lattice with divalent B-site cations within the six-fold coordinated cavities. B-X bonding of perovskite governs the electronic behavior of perovskite semiconductors while A cation has no direct role for the electronic properties. But the size of the A cation may cause the distortions in symmetry of the material. Besides the cubic phase, perovskite has tetragonal and orthorhombic phase also. For example, $MAPbI_3$ has a tetragonal structure while $MAPbBr_3$ and $MAPbCl_3$ have a cubic structure at room temperature. The symmetry of $MAPbI_3$ perovskite also depends on the temperature and symmetry increases with increase in temperature such as, at a lower temperature it has octahedral symmetry, and at room temperature to (162.2–327 K) has tetragonal white at a higher temperature above 178.8 K shows cubic phase. $FAPbI_3$ perovskite has higher symmetry than MA-based perovskites hence has been most widely investigated [19]. $FAPbI_3$ perovskite has nearly cubic structure at room temperature and inert atmosphere. At open atmosphere, FA shows its yellow phase that is non-perovskite phase of this material, and it is not useful for optoelectronic devices because of the high band gap.

This is the only drawback with FA material otherwise FA-based perovskite would exceed those of MA [20].

Every ABX_3 structure cannot be a perovskite phase. There is some fixed criteria for the existence of perovskite structure: (1) charge neutrality: that means the charges of cation and anion should be equal. For example, for ABX_3 structure, A and B cations have 1+, and 2+ charges (total = 3+) and X anion has 3− charges. So both cation and anion have equal costs, i.e., N(A) + N(B) = 3 N(X), here N belongs to the valence of the A, B and X ions; (2) the Goldschmidt tolerance factor, t and (3) octahedral factor μ. t and μ are the most potent factor that decides the existence and structure of the perovskite material. Tolerance factor t and octahedral factor μ are defined as the following equation:

$$t = \frac{(rA - rx)}{\sqrt{2}\,(rB - Rx)} \text{ and } \mu = \frac{rB}{rX}$$

where r_A, r_B, and r_X are the ionic radii of A, B, and X, respectively. For the perovskite structure, the value of t and μ must be lies between given limit; $0.89 < t < 1.11$ and $0.442 < \mu < 0.895$ [21]. Thus from the above formula, it is clear that the size of the A, B and X ions play an essential role for the perovskite materials. These days the Goldschmidt tolerance factor concept is beneficial for the finding the lead-free perovskite materials based on the ionic radii of implicated ions. Beside B-site replacement, there are too many possibilities of the other ion positions such as A as well as X-site. On the basis of this concept, Kieslich and co-workers have theoretically found out more than 600 hypothetical perovskites that have not been reported yet [22]. Such kind of study can help develop less lead of lead-free perovskite materials on the practical level for commercialization.

3. Optical properties of halide perovskite

Organic-inorganic perovskite materials demonstrate a strong optical absorption and bandgap tuning, long diffusion length, high charge carrier mobility, ambipolar charge transport and high tolerance of defects. Strong light absorbing properties of the material ideally suited for solar cell devices. On the other hand, band tuning properties and a wide range of light emission in the visible range with narrow emission bandwidth (FWHM) suitable for the light emitting devices. Organic-inorganic perovskite materials have sharp optical band edge that indicates the direct bandgap and minimal disordered materials [23]. The bandgap of perovskite material can be controlled by their chemical compositions and crystallite size. For example, $CH_3NH_3PbI_3$ (red emission), $CH_3NH_3PbBr_3$ (green emission) and $CH_3NH_3PbCl_3$ (blue emission) hybrid perovskites have band gap of 1.55, 2.3 and 3.1 eV, respectively [24].

The band gap energy levels of hybrid perovskite are determined by an anti-bonding hybrid state between the cation B-s and anion X-p orbitals. This state is related to the valance band maxima and conduction band minimum. Thus due to their unique ABX_3 structure and compositional flexibility, optical properties can be tuned by varying elements at each site. The change in I/Br ratio in $CH_3NH_3PbX_3$ perovskite can modify the bandgap from 1.55 to 2.3 eV, i.e., PL emission can be tuned red, orange and yellow. This band gap tuning mechanism is due to the hybridization of p and s orbitals such as Br-4p orbital is overlapped with the I-5p orbital and the Pb-6 s orbital. Similarly, with varying the concentration of Cl/Br, we can tune bandgap from 2.3 to 3.1 eV for hybrid perovskites [25]. Another approach is tuning of the band gap in perovskite structure is substitution of $(CH_3NH_3)^+$ site

(A) by Cs^+, Rb^+ or mixing of both Cs/other alkyl-ammonium cations. With changing the A cation, the bond length with B and X site is also changed that is responsible for the band gap tuning. $CsPbI_3$, $CH_3NH_3PbI_3$ and $FAPbI_3$ has band gap of 1.73, 1.55 and 1.48 eV, respectively [26]. So from these values, we can see that the band gap of the material decreases with increasing the cation size. Besides A and X site, the band gap energy can be tuned with changing the Pb^{2+} (B) from other divalent cations like Sn^{2+}, Mn^{2+}, Cd^{2+}, etc. [26].

Depending on the particle size, dimensions and morphology hybrid perovskite materials show different optical energy gap than their bulk counterparts due to their quantum confinement effect. For traditional nano-materials, quantum confinement effect has been widely studied. In recent times, the development of size-controlled perovskite QDs has enabled exhaustive research and developments of quantum confinement effect in QDs. Size of perovskite QDs can be controlled or tuned by ligand OLA. Friend et al. have studied on the size-dependent photon emission from $CH_3NH_3PbBr_3$ PQDs, where the particle size and the PL emission peak could be tuned by varying the concentration of the perovskite precursors [27]. Quantum confinement effects have also been reported by Kovalenko group in all inorganic $CsPbBr_3$ PQDs. They found that, with a decrease in the diameter of particle size from 11.8 to 3.8 nm, the PL emission peak gradually blue-shifted from 512 to 460 nm [28]. The thickness of the QDs also responsible for the band gap tuning. Thus trough band gap tuning, multi-colored LEDs and white LED can be formed by simple and easy way.

4. One step towards lead-free perovskite materials

Perovskite quantum dots are considered as the most capable aspirant to the next generation of optoelectronic devices and solar cells technology. But the presence of toxicity due to Pb restricts the commercialization. Hence, currently, most of the research is going on less lead or Pb-free perovskites. The nontoxic and environmentally free perovskite can be prepared by substituting Pb with nontoxic elements that can be achieved through two approaches, i.e., homovalent and heterovalent substitution. Homovalent elements for lead substitution with an isovalent cation such as Sn^{2+}, Mn^{2+}, Cd^{2+}, Zn^{2+}, etc. while heterovalent are aliovalent cations like Bi^{3+}, Sb^{3+}. In this work, we will only discuss homovalent cation substitution of PQDs.

4.1 Homovalent substitution

For the Pb-free perovskite materials, many homovalent elements with +2 stable oxidation states can be used. For example, the group- 14 elements Sn^{2+} and Ge^{2+}, i.e., the same group of Pb^{2+} can be the best choice for lead substitution. Beside this, transition metals as Cd^{2+}, Mn^{2+}, Fe^{2+}, Cu^{2+} and Zn^{2+}; alkaline-earth metals such as Ba^{2+}, Sr^{2+} and Ca^{2+}; rare-earth elements like Eu^{2+}, Yb^{2+} can be considered for the Pb-free perovskites [29]. Theoretically, these Pb-substitutes are perfect for perovskite structure according to the tolerance factor calculations. But some elements like Ba, Sr, and Ca have a large band gap, so these are not suitable for semiconducting materials. However, working with Cu and Zn in ambient condition will be difficult. In recent years, Sn^{2+} and Mn^{2+} are the promising candidates for homovalent substitution in perovskite quantum dots.

4.2 Sn-based perovskite quantum dots

The most suitable Pb-substitute is Sn^{2+} for lead-free perovskite because of the around same ionic radii, binding energy and the same electronic configuration of

s^2 valence [29]. $MASnI_3$ is the most studied lead-free perovskite material. Sn-based perovskites are direct bandgap semiconductors, like Pb-based perovskites. This means, the valence band maximum and conduction band minimum recline at the same position in k-space (reciprocal space). Similar to the $APbX_3$ structure, the structural, optical and electrical properties of $ASnX_3$ perovskite is also affected by the size of A-site cation and X-site anion. $MASnI_3$ perovskite also has a tetragonal structure, but the band gap is near unity that is lower than those of the $MAPbI_3$ [30]. Due to the quantum confinement effect, PQDs shows different behavior from their bulk counterpart.

In case of the pure inorganic perovskite $CsPbI_3$, band gap of PQDs is 1.85–1.97 eV. Such kind of higher bandgap highly encouraged to find some lower Pb-containing, low band gap, and more stable perovskite material. $CsSnI_3$ pure inorganic can be the satisfied the all requirements for the good PQDs because of its lower binding energy and broad absorption from visible to near infrared region. Due to this different behavior, such kind of perovskite can exhibit higher light harvesting efficiency than other perovskite materials [31]. However, the stability of the Sn^{2+}-based perovskite material is the biggest issue due to higher sensitivity to air, moisture and sometimes with nonpolar organic solvents also [32]. In recent years, many significant approaches have been tried for the stability of the Sn^{2+} perovskites. For example, $SnBr_2$, $SnCl_2$, and SnF_2 had used as a dopant into the $CsSnI_3$ perovskite for the stability of the materials. In all, depends, SnF_2 and $SnCl_2$ were found more suitable for the air resistive property. However, stability of the Sn-based material was not satisfactory due to the degradation of the sample within only 3hs [33–35].

In the year 2017, Liu et al. reported, the alloyed $CsSn_{1-x}Pb_xI_3$ PQDs, which was more phase stable than its parent $CsPbI_3$ and $CsSnI_3$ PQDs for months in ambient air [36]. They have prepared $CsSn_{1-x}Pb_xI_3$ PQDs via the standard Schlenk line method under a nitrogen atmosphere. In this method, SnI_2/PbI_2 mixture was rapidly dissolved in trioctylphoshine into the cesium olate at 120–170°C and purified by antisolvent methyl acetate (MeOAc) washing process. The 140°C reaction temperature was found the best for homogeneous and proper morphology of $CsSn_{1-x}Pb_xI_3$ PQDs. With the incorporation of Sn, red shifting occurred that can be observed in absorption and PL spectra as shown in **Figure 1a**.

Additionally, the increase in Sn concentration drastically enhanced the light absorption of $CsSn_{1-x}Pb_xI_3$ PQDs; however, PLQY was found up to 3% only. On the other hand, $CsPbI_3$-based PQDs had up to 100% efficiency to date. Low PLQY with Sn-based PQDs indicates the increase in intrinsic defects that were allied with Sn vacancies. Such kind of vacancies creates deep level defects which act as non-radiative recombination centers and hence this reduces the efficiency of PQDs. **Figure 1b** also suggested the average lifetime of $CsSn_{1-x}Pb_xI_3$ PQDs dramatically decreases with increasing the concentration of Sn. This behavior of Sn containing materials also confirms the occurrence of a large density of quenching defects that support the lower PLQY of the PQDs. Liu also reported that $CsSn_{0.60}Pb_{0.40}I_3$ PQDs was best for performance and stability because of the less- Pb content and widest range of light absorption among the alloyed PQDs. Phase, as well as chemical Stability of $CsSn_{0.60}Pb_{0.40}I_3$ PQDs, is confirmed via XRD and XPS analysis (see **Figure 1c** and **d**). XRD **Figure 3b** suggested that there is no degradation was absorbed up to 5 months that is the first time reported such long time stability with Sn-based material.

Furthermore, there was not found Sn^{4+} oxidation stage in the XPS analysis of the sample. In **Figure 1d** XPS graph showed 2 spectra at 486.2 and 494.5 eV that is associated with Sn^{2+} $3d_{5/2}$ and $3d_{3/2}$ state, while deficiency of spectra at 486.9 indicates the absence of Sn^{4+} in perovskite compound. Thus this less lead-containing and air-stable Sn-based PQDs can be the best choice for solar cell devices but for highly

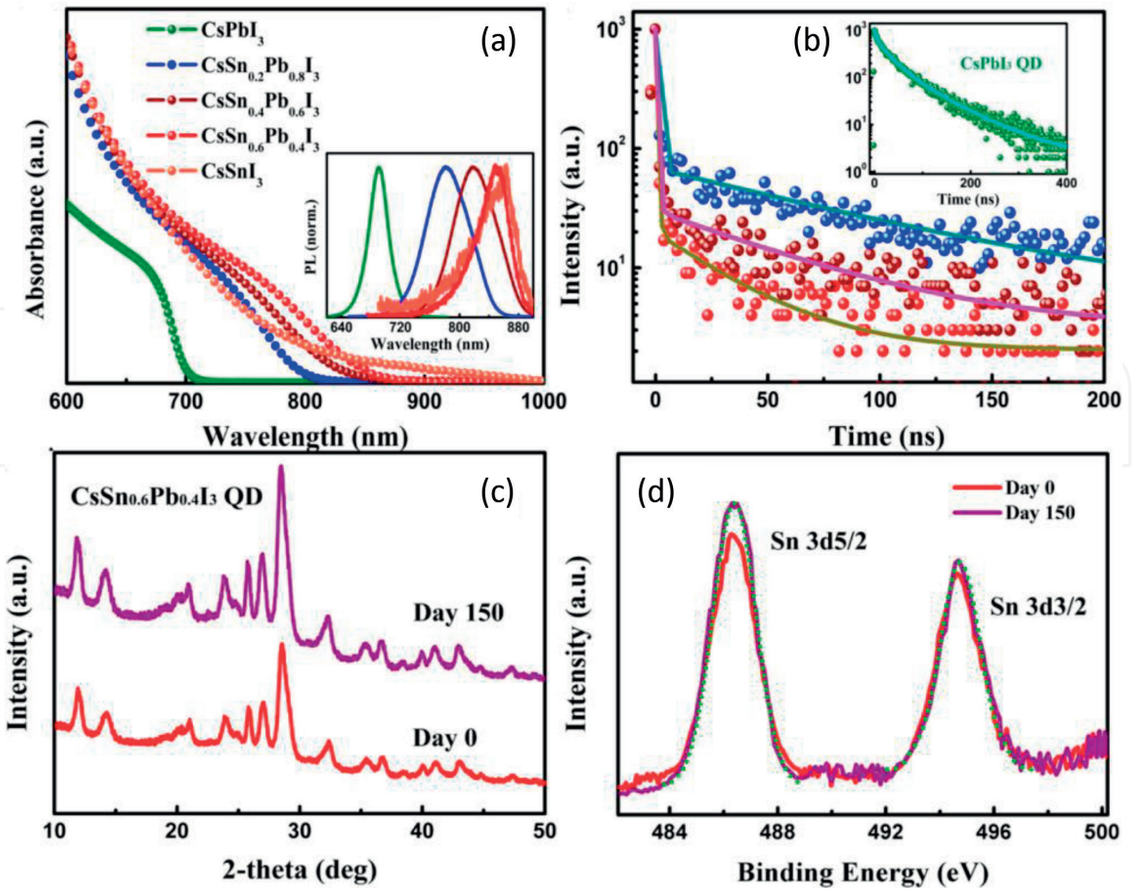

Figure 1.
(a) Optical absorption spectra of different Sn doped PQDs and the inset fig shows their corresponding normalized steady photoluminescence spectra, (b) time-resolved photoluminescence decay for various stoichiometries of Sn, (c) X-ray diffraction patterns and (d) XPS spectra for the $CsSn_{0.60}Pb_{0.40}I_3$ PQDs (as prepared) and those after storage for 150 days.

efficient LED there will be a need in the improvement of its PLQY. Jellicoe and co-workers had also tried for the Sn-based perovskite, $CsSnX_3$ (X = Cl, Br, I) for the lead-free perovskite PQDs but due to the instability of Sn it cannot be used for practical applications [35]. To overcome the stability problem, Wang group had replaced Sn^{2+} with Sn^{4+} and developed stable $CsSnI_6$ PQDs with cubic structure. However it's PLQY was just 0.48% that is also not sufficient for optoelectronic applications [36]. From the several studied we absorbed that, $CsSnI_3$-based perovskites have low PLQY but good hole conducting properties. Hence it is mostly used for solar cell applications. For sufficient PLQY and more stable Sn-based material was still needed for display devices. For this purpose, $CsSnBr_3$-based perovskite was found more suitable candidate than iodine-based perovskites.

Yang group have reported the fast and less Pb or Pb- free perovskite nanocrystals by introducing the Sn in Pb site and I at Br site [37]. They have used one pot hot injection method for preparation of SnI_2 doped $CsPbBr_3$ perovskite nanocrystals. After cation and anion exchange between the $CsPbBr_3$ and SnI_2, the lead-free $CsSnI_3$ NCs were obtained. These Pb-free NCs maintained the high PLQY as well as morphology in an inert atmosphere. **Figure 2a** indicated that, with increasing the amount of SnI_2 into $CsPbBr_3$ colloidal solution, dramatically red shifting observed in PL emission and absorption spectra. There was one fascinating result was reported regarding the stability of Sn^{2+}. XRD result predicted that Sn^{2+} converted into Sn^{4+} and formed the small amount of Cs_2SnI_6 phase that indicated the cation as well as anion exchange in the sample. After cation exchange between Pb^{2+} and Sn^{2+} and anion exchange between Br^{-1} and I^{-1}, the PLQY of $CsSnI_3$ and $CsPbBr_3$ NCs was

found 59.1 and 73.47% respectively. From this result, the author concluded that the ion exchange did not cause the structural and surface defects. **Figure 4b** shows the schematic representation of the cation and anion exchange in $CsPb_xSn_{1-x}(Br_yI_{1-y})_3$ NCs. Halide anions have high migration and the sufficient vacancy diffusion ability that is why after incorporation of SnI_2 into $CsPbI_3$, halide anions reacts very fast [38]. On the other hand, cation takes more time to reaction with parent material due to the obligation of high activation energy. Moreover, in most of the cases, cation substitution is obsessed with the concentration of halide vacancies [39]. Thus with this cation and anion approach creates a possibility of higher PLQY of Pb-free perovskite NCs.

The 100% Pb replacement with any other divalent cation is impossible till date because of the lower conductivity of substitute element like Sn. In the case of the Sn lower ionic conductivity of PQDs causes many surface defects that make material unstable. Some of the Pb-free perovskite with Sn^{4+} support that instability and toxicity problem can be resolve by partial substitution of Pb^{2+} with Sn^{4+}. In this regards, Liu et al. have reported the less lead-containing $CsPb_{1-x}Sn_xBr_3$ PQDs with PLQY up to 83% [40]. They have performed cation exchange via replacing Pb^{2+} cation with Sn^{4+} cation using hot injection method. Partial replacement with Sn^{4+} in $CsPb_{1-x}Sn_xBr_3$ exhibited the enhancement in PL emission and after some time increasing the more concentration of Sn^{4+} ion, decreases the PL performance due to the increasing the impurity phase of Cs_2SnBr_6. In this work, they found $CsPb_{0.67}Sn_{0.33}Br_3$ was the best composition, and PQDs of material, displayed the high external quantum efficiency and current efficiencies. **Figure 3a** Shows the variation of PL spectra of $CsPb_{1-x}Sn_xBr_3$ PQDs and digital picture in UV irradiation (365 nm). This PL spectrum show the highest PL intensity for x = 33% while increasing the concentration of Sn; PL intensity starts to decrease due to impurity and more surface defects. **Figure 3b** shows the absorption and PL emission spectra of samples that indicated the absence of blue shift that means there is no big effect on band gap after Sn^{4+} incorporation, but exciton recombination can affect the

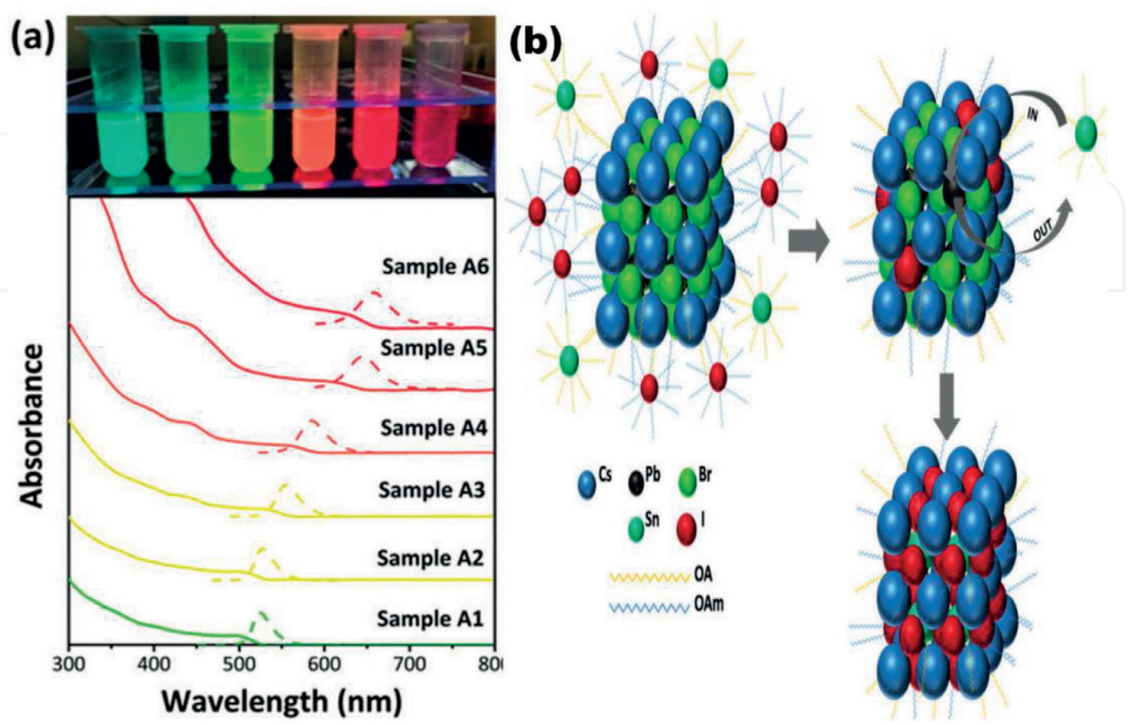

Figure 2.
(a) UV-Visible and PL spectra of different Sn doped $CsPbBr_3$ NCs (A1–6); the colored image of PQDs under 365 nm UV radiation and (b) schematic diagram of the ion exchange process in SnI_2 doped $CsPbBr_3$ NCs.

lifetime and lower PLQY with a higher concentration of Sn^{4+}. A higher concentration of Sn^{4+} also affected the size; morphology and structure of the QDs (see **Figure 3c–g**). After x = 0.33 Sn^{4+} amount in $CsPbBr_3$, the impure phase can be seen in the XRD spectrum and irregular shape and agglomerated particles in TEM due to Cs_2SnBr_6 byproduct.

4.3 Mn^{2+}-based perovskite QDs

Mn^{2+} is a transition metal cation, and doping of Mn^{2+} in II-VI semiconductors has been widely investigated due to its excellent optical, electrical and magnetic properties. All ready many studied have been done on Mn^{2+} doped ZnS, CdSe, CdS, and ZnSe inorganic QDs in which Mn^{2+} incorporation can enhance the long-lifetime and interaction between host d-electron of Mn dopants [41]. In compare to the traditional II-VI group semiconductors, the soaring tolerance in perovskite can be the better candidate for promoting the exciton energy transfer to Mn d-d emission to Mn d-state.

The band gap of Mn^{2+} doped in perovskite materials depends upon the presence of halide anions in a host as well as a dopant. For example, change from Cl^- to Br^- to I^-, the PL emission of perovskite is tuned from blue region to red. In the year 2018, Zhao et al. have reported the Mn^{2+} doped $CsPbCl_3$ NCs and after that intensive exploration are carried on this work [42]. After incorporation of Mn^{2+}

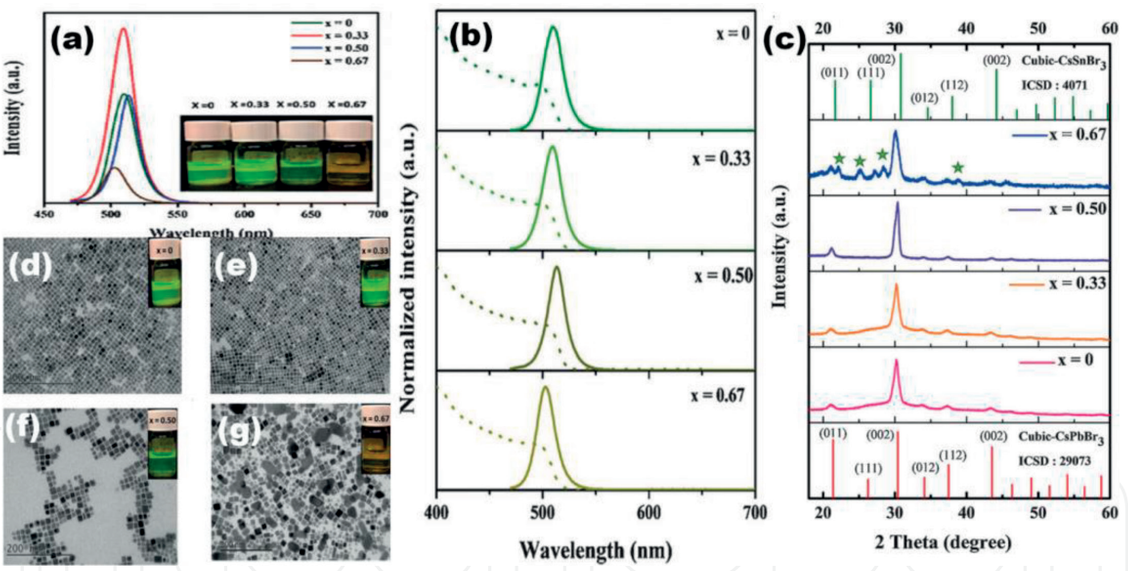

Figure 3.
(a) Variation in PL intensity of different Sn^{4+} doped $CsPbBr_3$ PQDs. Inset of samples under 365 nm UV light (b) UV-Visible absorbance and PL spectra of $CsPb_{1-x}Sn_xBr_3$ (c) XRD pattern of $CsPb_{1-x}Sn_xBr_3$ PQDs, impurity peaks are shown by stare sign. (d–g) TEM images with (d) x = 0, (e) x = 0.33, (f) x = 0.50 and (g) x = 0.67.

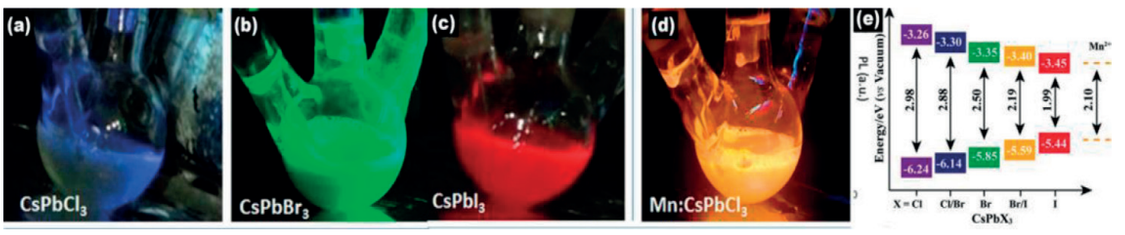

Figure 4.
(a–d) Digital images of $CsPbCl_3$, $CsPbBr_3$, $CsPbI_3$ and Mn: $CsPbCl_3$ nanocrystals under 365 nm UV radiation and (e) band positions of $CsPbX_3$ and Mn^{2+} d-state.

cation in place of Pn^{2+} site, the XRD spectra shied towards higher angle due to the smaller radii of Mn^{2+} while PL emission shifted towards higher wavelength because of the d-d transition. Hence undoped $CsPbCl_3$ NCs shows blue emission, but after doping of Mn^{2+}, it tuned into orange emission as shown in **Figure 4a–c**. It was reported that Cl-based Mn dopant and perovskite host is the best rather than other manganese (II) salts [43]. Via hot injection method, it is tough to doping of Mn^{2+} into $CsPbBr_3$ and $CsPbI_3$ perovskite structure but through the anion exchange process Mn doping is possible. Such kind of possibility depends upon the bond strength and dissociation energy between Mn-X and Pb-X bond. **Figure 4d** shows the band gap energy diagram for Mn-doped different perovskite host [44]. As we know Cl-based perovskite NCs has very low PLQY (<5%) in compared to Br- and I-based perovskites. Besides reduction in toxicity, Mn^{2+} doping helps to enhance the PLQY and lifetime of the perovskite NCs. In this regards, Liu and coworkers fabricated $CsPb_xMn_{1-x}Cl_3$ PQDs via hot injection method [45]. Mn^{2+} incorporation in $CsPbCl_3$ not only increases the PLQY of host material from 5 to 54% but also created an additional intense PL emission peak at 580 nm that is stand for bright orange color (see **Figure 5a**). With increasing the Mn^{2+} concentration secondary, PL peak gradually shifted from 569 to 587 nm. The highest PLQY (54%) was found for the 46% Mn-doped $CsPbCl_3$ perovskite. The various Mn^{2+} compositions with tunable emission are shown in schematic **Figure 5b**. $CsPb_xMn_{1-x}Cl_3$ PQDs has two emission peaks with two different lifetime values such as 13.9 ns at 390 nm and 1.6 ms at 580 nm as shown in **Figure 5a** and **b**. The long decay time for second emission peak near 580 nm is assigned to emission from d-d transition energy transfer mechanism for Mn^{2+} doped semiconductors. Hence Mn^{2+} doping also increases

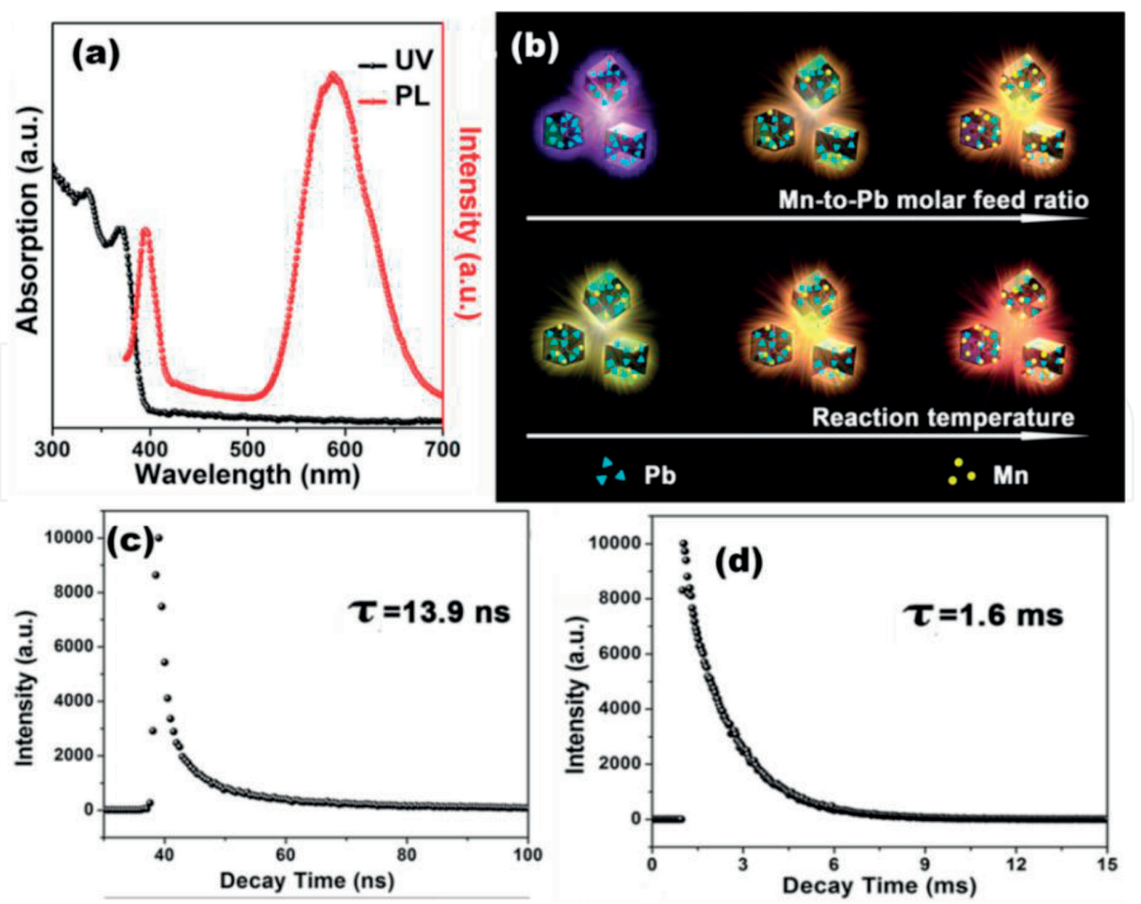

Figure 5.
(a) UV-Visible and PL spectra of $CsPb_{0.54}Mn_{0.46}Cl_3$ PQDs (b) schematic illustration of Mn incorporation in $CsPbCl_3$ PQDs by different molar ratio and reaction temperature, (c and d) PL lifetime of $CsPbCl_3$ and $CsPb_{0.73}Mn_{0.27}Cl_3$ PQDs.

the overall lifetime of PQDs that may be an improvement in the stability of PQDs also. A similar study was carried by Yuan et al. in which they have obtained PLQY of up to 60% for 14.6% Mn^{2+} doped $CsPbCl_3$ [46]. With the help of ligand assisted room temperature method (LART), same work was reported by Zhu group with maximum 41.6% PLQY for 28% Mn^{2+} incorporation in place of Pb^{2+} [47]. Through LART, Mn^{2+}:$CsPbCl_3$ can be prepared in concise time duration and room temperature that reduce the cost of experiment, easy, simple method and high production of products.

In some cases, Mn^{2+} is beneficial for stability of $CsPbX_3$ PQDs. Zou et al. have found that Mn^{2+} incorporation in place of Pb^{2+} not only reduced toxicity while also enhance the thermal as well as air stability of the perovskite samples [48]. Similar to previous work, Zou group also have worked with $CsPbCl_3$: Mn^{2+} PQDs and studied different structural and optical enhanced properties. Besides this work, they have also provided experimental data for $CsPbBr_3$: Mn and $CsPbI_3$: Mn PQDs to prove the absence of energy transfer in Br and I containing perovskites. **Figure 6(a–c)** show the comparison of PL spectra for $CsPbCl_3$: Mn, $CsPbBr_3$: Mn and $CsPbI_3$:Mn PQDs with various Mn^{2+} concentrations. In this case, PL emission intensity first increases with increasing the Mn^{2+} concentration and then decreases with further increasing doping concentration which suggests that the Mn^{2+} ions have a noteworthy impact on the optical properties of PQDs. Presence of additional peak in $CsPbCl_3$: Mn, is the proof of energy transformation, on the other hand, there is no peak shift in Br and I containing PQDs samples due to the mismatch between their optical bang gap absorption and $^4T_1 \rightarrow {}^6T_1$ transition of Mn^{2+} [48]. PLQYs of the Cl-based increases and in Br and I increases up to 20% Mn^{2+} doping and after that dramatically decreases with increasing the Mn^{2+} concentration (see **Figure 6d–f**) while lifetime of $CsPbBr_3$: Mn^{2+} continuously decreases as shown in **Figure 6g**. Mn^{2+} doping in $CsPbBr_3$ and $CsPbI_3$ PQDs also enhance air stability as demonstrated in **Figure 6h** and **i**. **Figure 6h** indicates, the degradation of pure $CsPbBr_3$ PQDs after 30 days while Mn^{2+} doped PQDs is stable up to 120 days while 50%Mn: $CsPbI_3$ PQDs was found stable up to 4 days. As we know $CsPbI_3$ PQDs are unstable in the air, so it is challenging of use for optoelectronic devices. Enhanced stability of Mn: $CsPbI_3$ materials may open the new door for stable red PQDs. The same methodology was reported by Manna group by theoretical and experimental approach also [49]. They reported that unstable $CsPbI_3$ perovskite could be stabilized by incorporation the 10% of Mn^{2+} and there were no major changes in structural and optical properties.

4.4 Cd^{2+} and Zn^{2+} doped perovskite quantum dots

Cd and Zn^{2+} Cation exchange in traditional NCs have been extensively studied, but for perovskite material, there are few reports are present till date. A detailed study of cation exchange has not yet been explained, but halide exchange has been explained well. Halide exchange is easier than cation exchange because of low activation energy and diffusion of anion vacancies in the perovskite materials. Stam et al. have experimentally proved that cation exchange in perovskite takes long time [50]. They reported the cation exchange such as Sn^{2+}, Cd^{2+}, and Zn^{2+} in place of Pb^{2+} in $CsPbBr_3$ perovskite host. 10% cation exchange in perovskite system results in the reduction in toxicity due to lead and also maintained the good PLQY as well as high color purity. But with these, cation exchange, the blue shift was observed in PL emission due to smaller ionic radii of Cd and Zn than Pb (as shown in **Figure 7k**). On the other hand, there is very less shift was obtained in Sn^{2+} due to similar ionic radii as Pb. The Cd^{2+} doping in $CsPbBr_3$ PQDs was resulting in PL emission variation between 452 and 512 nm while Zn showed between 462 and 512 nm. Furthermore, over 60% of PLQYs was obtained for cation doped PQDs and good

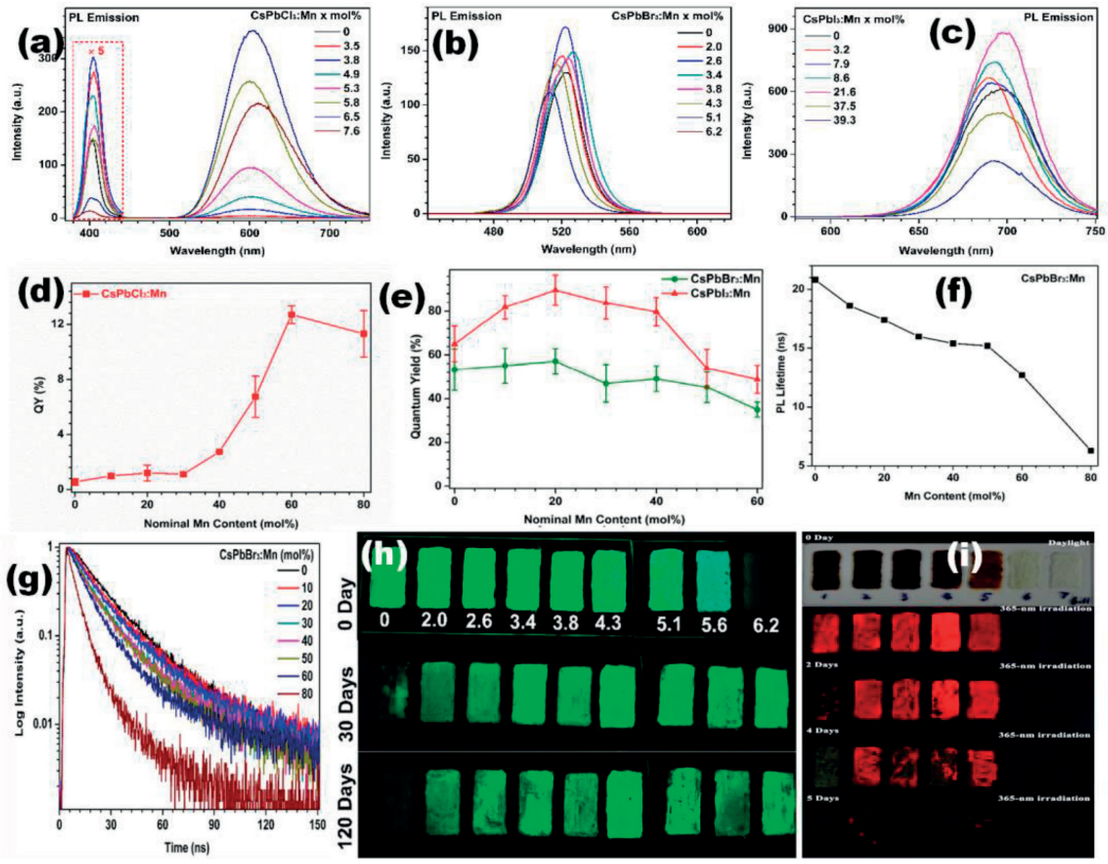

Figure 6.
Comparison of photoluminescence (PL) emission spectra for (a) $CsPbCl_3$:Mn, (b) $CsPbBr_3$:Mn and (c) $CsPbI_3$:Mn QDs doped with different Mn^{2+} contents (d) absolute PL quantum yields (QYs) for $CsPbCl_3$:Mn QDs doped with different nominal Mn^{2+} contents ranging from 0 to 80 mol% (e) absolute PL QYs for $CsPbBr_3$:Mn and $CsPbI_3$:Mn QDs doped with different nominal Mn^{2+} contents ranging from 0 to 60 Mol% (f and g) PL decay curves (left) and lifetimes (right) for excitonic luminescence of $CsPbBr_3$:Mn QDs upon excitation by a 397-nm pulsed laser (h) PL emission photographs for $CsPbBr_3$:Mn QDs coated on the surface of a glass slide with different Mn^{2+} contents from 0 to 6.2 mol% taken under UV irradiation at indicated time periods and (i) red PL emission photographs for $CsPbI_3$:Mn QDs with different nominal Mn^{2+} doping concentrations of 0, 20, 40, 50, 60, 80, 100 mol% from left to right respectively, taken at daylight or under UV irradiation at indicated time period.

stability in ambient conditions. Cation exchange in PQDs reduced the PL lifetime of the $CsPbBr_3$ PQDs. **Figure 7a–j** TEM and energy dispersive X-ray spectroscopy mapping of Cd^{2+} and Zn^{2+} doped $CsPbBr_3$ PQDs. EDS mapping helped to identify the presence of different doped elements in PQDs. **Figure 7a–e** shows the Cd and **Figure 7f**-jshows the Zn doped $CsPbBr_3$ PQDs. These mapping analyses also predicted the uniform distribution and lower concentration of dopant into the host material. Zn^{2+} incorporation enhanced the stability of $CsPbI_3$ black phase in the air also due to improvement in lattice contraction and alloy form of perovskite.

As it is well reported that lower PLQYs of Cl-based perovskite materials due to the large band gap. There are many have published on Mn^{2+} doped $CsPbCl_3$ PQDs, but with doping of, we get orange color so in this case to obtain pure blue color is impossible. On the other hand, other heterojunction-based PQDs such as $CH_3NH_3Bi_2X_9$, $Cs3Bi_2Br_9$ and $Cs_3Sb_2Br_9$ have been developed for blue emission [50]. But still, these blue color emitted PQDs have 46–52% and very unstable that is not suitable for blue LEDs fabrication. To overcome this issue, Mondal et al. reported the effect of Cd incorporation in $CsPbCl_3$ PQDs by hot injection method to enhance the stability and PLQYs of blue color PQDs [51]. For $CdCl_2$ treatment, $CsPbCl_3$ colloidal solution with $CHCl_3$ was mixed with $CdCl_2$ solution ($CdCl_2$ solution was prepared in ethanol) and sonicated for 2–3 min. The obtained colloidal solution was

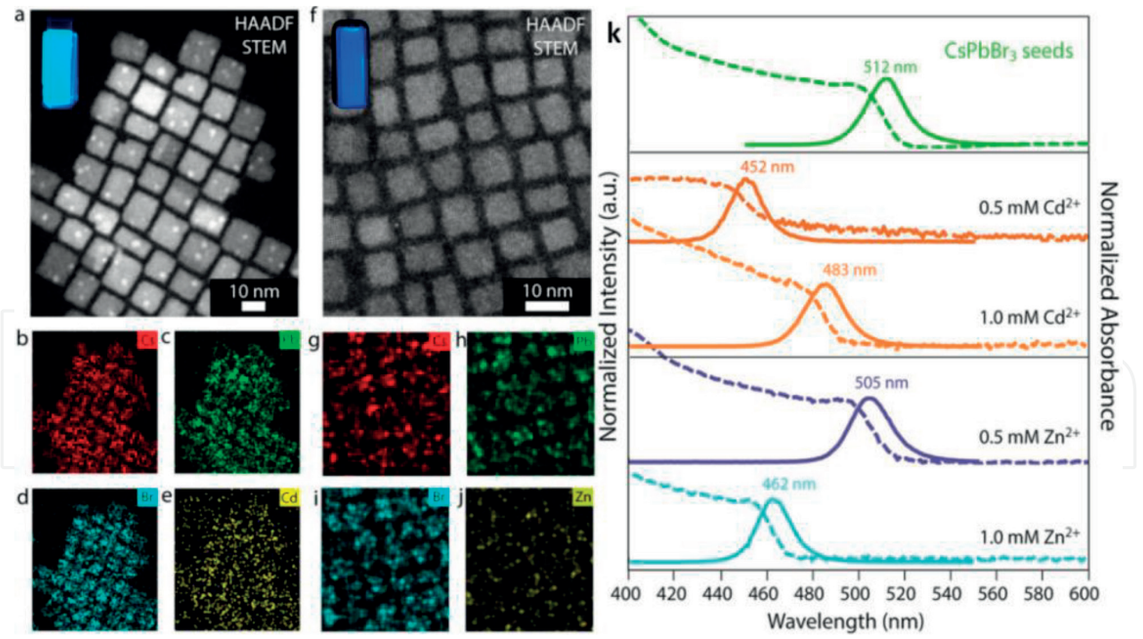

Figure 7.
Energy dispersive X-ray spectroscopy mapping of $CsPb_{1-x}Cd_xBr_3$ and $CsPb_{1-x}Zn_xBr_3$ nanocrystals. (a) HAADF-STEM image of $CsPb_{1-x}Cd_xBr_3$ NCs and corresponding maps of (b) Cs, (c) Pb, (d) Br, and (e) Cd, demonstrating the presence of Cd in the perovskite NCs. The inset in panel shows a photograph of a colloidal suspension of the NCs under UV illumination. (f) HAADF-STEM image of $CsPb_{1-x}ZnxBr_3$ NCs and the corresponding maps of (g) Cs, (h) Pb, (i) Br, and (j) Zn, indicating the presence of Zn in the perovskite NCs. The inset in panel f shows a photograph of a colloidal suspension of the NCs under UV illumination (k) parent $CsPbBr_3$ NCs (green lines) and product NCs obtained after reaction with different concentrations of $CdBr_2$ (orange lines) and $ZnBr_2$ (blue lines).

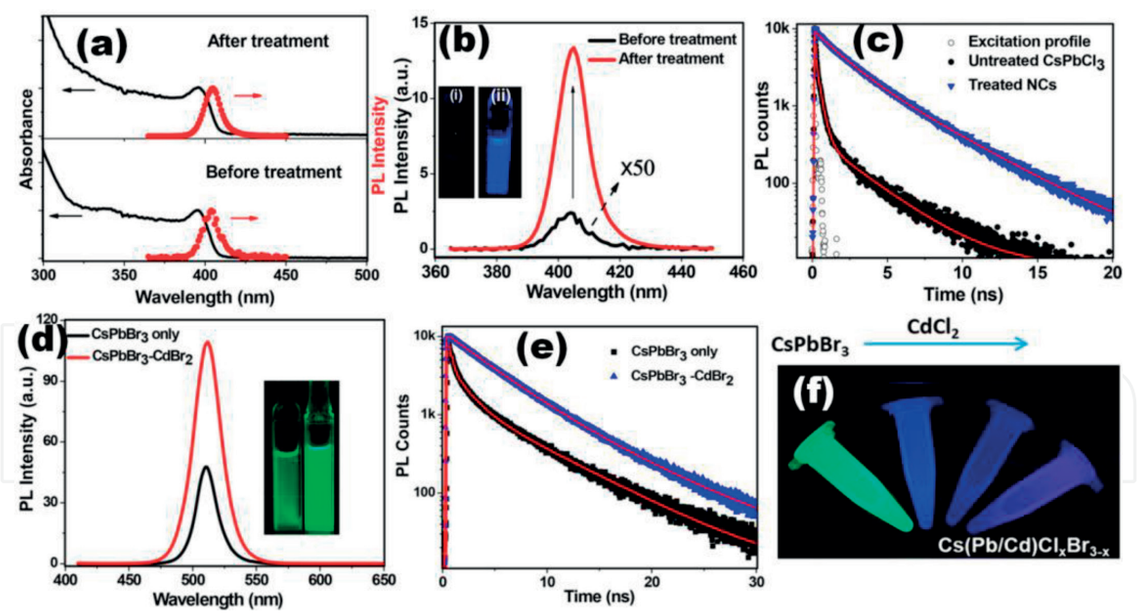

Figure 8.
UV-Visible absorption and PL spectra (a) of the $CsPbCl_3$ NCs before and after the $CdCl_2$ treatment. PL spectra showing dramatic enhancement of PL upon treatment (b) the inset shows the untreated (i) and treated samples (ii) under a UV lamp. (c) PL decay dynamics (λ_{ex} = 375 nm, λ_{PL} = 406 nm) of $CsPbCl_3$ NCs before and after the treatment with $CdCl_2$. PL spectra (d) and PL dynamics (e) of $CsPbBr_3$ NCs before and after the CdBr2 treatment. (f) Change in PL on addition of $CdCl_2$, starting from treated $CsPbBr_3$ NCs (left) to increased addition of $CdCl_2$ (right).

purified by centrifugation with methyl acetate treatments. The $CdCl_2$ treatment of $CsPbCl_2$ dramatically enhanced the from 3–96% PLQYs and narrow PL emission spectra that also indicates the higher color purity of the treated sample.

There are the best thing is that there was no PL or absorbance spectrum shifting observed with $CdCl_2$ treated samples as shown in **Figure 8a**. From **Figure 8b** also indicates the huge improvement in PL emission and bright blue emission under UV light radiation compared to untreated $CsPbCl_3$ PQDs. Generally, with doping of Cd^{2+} or other lower atomic radii elements than Pb^{2+}, has PL emission shift towards blue region due to lower ionic radii. But in this work, the authors did not get any shifting. $CdCl_2$ incorporation not only enhances the PLQYs while it also improved the lifetime and stability of $CsPbCl_3$ PQDs by the four times of the untreated PQDs (**Figure 8c**). A similar strategy was applied with $CsPbBr_3$ PQDs and improvement in PLQY and lifetime also absorbed in green PQDs also (**Figure 8d–f**). Thus this work suggests the Pb^{2+} cation exchange with Cd^{2+} not only provide high PLQYs while long term stability without disturbing any peak shifting. So such kind of blue and green PQDs can be beneficial for good quality of blue, green or white LEDs and a backlight system. Thus Cd and Zn doped PQDs may be useful for different optoelectronic applications similar to pure PQDs due to its low toxicity and excellent properties.

5. Applications of lead substituted PQDs for LEDs

Lead halide-based perovskite QDs, as a promising light-harvesting material for light absorbing and converting light energy, have attracted research community as well as industrialists due to unique properties of PQDs for solid-state lighting (SSL) and flexible color tuning thin film display application. In recent years, organic LED (OLED) and quantum dot LED (QDLED) join the competition of display market and mean to wrest the dominance from LCD. OLED has the advantage of self-luminous, large area fabrication, fast response time, high contrast and application on flexible substrates [2–4]. Due to such type of benefits, many manufacturers have invested in the development of OLEDs, and now various products based on OLEDs have been commercially available. However, there are some limitations with OLEDs like wide PL emission wavelength, instability of organic molecules, etc. Due to this issue, it is difficult to achieve high color purity and a high-quality full-color display. So it is still required to develop a new variety of display technology with high color purity and PLQY to meet the higher demand of consumers. To overcome the less color purity problem, quantum dots can be used because of its excellent luminescence and color characteristics as we have already discussed in the previous section. There is a chance to achieve the high-resolution color contrast and a better full-color display device in near future moreover in contrast to another semiconductor (inorganic) employed in solid state lighting device perovskite material have also benefited regarding the synthesis and manifesting process. PQDs can also fabricate at low temp, solution processed approach to precisely control the size, shape, and purity of perovskite material which makes PQDs ideal candidates for the display device. In addition, due to the colloidal solution characteristics, PQDs is cheaper to use, easier to process and easier to fabricate in large area, large scale production thus PQDs are often touted as disruptive material that could completely replace traditional inorganic phosphor LEDs or OLEDs, QLEDs can be mainly divided into types one is photoluminescence QD LEDs (based on photoexcited), and another is electroluminescence (EL) QDLEDs (electron- excited QDs) [3]. PL QDLEDs is the most commonly used a type of LEDs. QDs LEDs usually have applications in the high-quality display, high resolution, and high contrast display device as well as in lighting application. For commercialization, much less lead-containing perovskite QDLEDs have been investigated in recent years. Lead substituted perovskites also used for PL LEDs and electroluminescence LEDs. Zou

et al. fabricated the EL-based LEDs using $CsPbBr_3$: Mn perovskite QDs [48]. Active LEDs was fabricated by spin coating of PEDOT: PSS on ITO glass substrate as a hole transporting layer, Mn-doped $CsPbCl_3$ as the active layer and TPBi, LiF/Al were used as electrodes by thermal evaporation technique. The schematic illustration of the device is shown in **Figure 9a**. This active led produced electroluminescence with green color (512–515 nm) for $CsPbBr_3$ and Mn-doped perovskites with high color purity and narrow emission spectrum FWHM of 20 nm (see **Figure 9b**). There were no significant shifting observed in EL as well as in current density-voltage properties (**Figure 9c**) of Mn-doped perovskites. Mn doping enhanced the luminescence of LEDs by 1.3 times of the pure PLEDs and EQE and CE also improved from 0.81% and 3.71 cd/A for the $CsPbBr_3$ PLED to 1.49% and 6.40 cd/A for the 3.8 mol% Mn-doped $CsPbBr_3$ PLED device. Similarly, Liu group also fabricated lead substituted active PLEDs with doping of 33 mol% Sn^{4+} ion consisting of the same device structure as Zou reported [40]. They reported that the presence of Sn^{4+} helped in the easy injection of charge carriers that is responsible for small turn off voltage as well as large current density. $CsPb_{0.67}Sn_{0.33}Br_3$ PLEDs showed 4.13% EQE, 12500 cd m^{-2} luminescence, 11.63 cd A^{-1} of CE, 6.76 lm W^{-1} and 3.6 V turn-on voltage. Authors have also claimed that such kind of high performance is the best results found in Sn-based PLEDs. So this lead substituted Sn-based PQDs LED can be suitable for different active LEDs as well for backlight-based display devices. On the other hand, $CsPbCl_3$: Mn PQDs has also been fabricated in PLEDs with 2.2 lm W^{-1} of luminous intensity (**Figure 9d–f**) and good stability after continuous applying 3.5 V of voltage for 200 h [45]. 27 mol% Mn: $CsPbCl_3$ was mixed with curable resin and coated on 365 nm commercial UV-LED chip for the PL PLED device. Due to d-d transition, Mn doped $CsPbCl_3$ PLED gives bright orange emission with 54% PLQY in ambient conditions. In most of the optoelectronic devices, photo and thermal

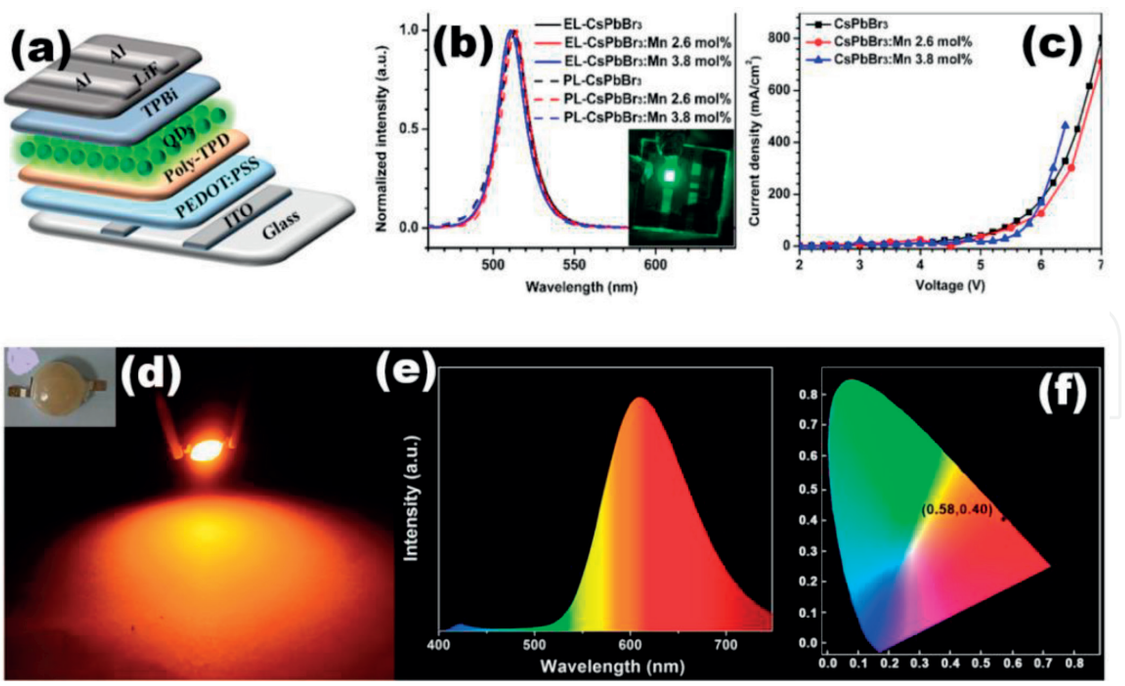

Figure 9.
(a) Schematic illustration of a typical multilayer-structured PLED device by using pure $CsPbBr_3$ and $CsPbBr_3$: Mn (2.6 mol%) and $CsPbBr_3$: Mn (3.8 mol%) QDs are used as green light emitters. (b) Comparison of normalized EL spectra at an applied voltage of 6 V and their corresponding PL emission spectra for $CsPbBr_3$ and $CsPbBr_3$: Mn (2.6 mol%) and $CsPbBr_3$: Mn (3.8 mol%) QDs when dispersed in cyclohexane solution. The inset shows a photograph of the EL of a representative PLED device. Current density (c) and luminance characteristics for three types of PLEDs based on the pure $CsPbBr_3$ and $CsPbBr_3$: Mn (2.6 mol%), and $CsPbBr_3$: Mn (3.8 mol%) QDs (d) fluorescent image (e), PL emission spectrum (f) CIE chromaticity coordinate of the LED from $CsPb_xMn_{1-x}Cl_3$ QDs. Inset: Optical image of the LED.

stability are the crucial issues. So for improving such kind of stability SiO_2 coating and KCl/polystyrene or other inorganic materials has been used for encapsulation of perovskite LEDs [42].

6. Summary

Lead halide-based perovskite material opens a new opportunity in optoelectric since 2012, because of their excellent optoelectronic properties and high power conversion efficiency within a brief time. The big challenge for the perovskite QDs is the presence of toxicity due to lead. Already many groups have worked on leadless or lead-free perovskite materials. 100% replacement of Pb will be complicated but with replacement up to 60–70%, Pb with non-toxic cation may help to the commercialization of less lead-containing perovskite materials. Shortly, less lead or lead-free PQDs have the potential for next-generation optoelectronic devices like backlights, QD TV, flexible and wearable devices, etc. However, to achieve high PLQY, good performances, and stability of lead-free or less lead containing PQDs also be challenging for the research community. Many homovalent lead substitutions like Sn, Mn, Cd, and Zn have been successfully done in place of Pb in different halide containing perovskite nanomaterials. Such kind of replacement of lead not only reduces the toxicity of perovskite while it also improves the performances and stability of the perovskite light-harvesting material. In the halide-based perovskites, dopant engineering is a compelling strategy to tuning the optical, structural, and electrical properties and day by day new depends arrive that make the PQDs more suitable for lead-free perovskite devices. Mn and Cd incorporation in Cl-based perovskite NCs was increased the PLQYs but for Br- and I-based PNCs it is still challenging to get high PLQYs than pure PQDs. So, we need to find a more suitable strategy for less lead-containing high PLQYs perovskite material.

Author details

Rajan Kumar Singh[1*], Neha Jain[1], Sudipta Som[2], Somrita Dutta[3], Jai Singh[1] and Ranveer Kumar[1]

1 Dr. Harisingh Gour Central University, Sagar, MP, India

2 National Taiwan University, Taipei, Taiwan (Republic of China)

3 National Chiao Tung University, Hsinchu, Taiwan

*Address all correspondence to: rajanphysicssgo@gmail.com

References

[1] Noh JH, Im SH, Heo JH, Mandal TN, Seok SI. Chemical management for colorful, efficient, and stable inorganic-organic hybrid nanostructured solar cells. Nano Letters. 2013;**13**:1764-1769

[2] Kojima A, Teshima K, Shirai Y, Miyasaka T. Organometal halide perovskites as visible-light sensitizers for photovoltaic cells. Journal of the American Chemical Society. 2009;**131**:6050-6051

[3] Guerrero A et al. How the charge-neutrality level of interface states controls energy level alignment in cathode contacts of organic bulk-heterojunction solar cells. ACS Nano. 2012;**6**:3453-3460

[4] Yang X et al. Author correction: Efficient green light-emitting diodes based on quasi-two-dimensional composition and phase engineered perovskite with surface passivation. Nature Communications. 2018;**9**:1169

[5] Schmidt LC et al. Nontemplate synthesis of CH3NH3PbBr3 perovskite nanoparticles. Journal of the American Chemical Society. 2014;**136**:850-853

[6] Kovalenko MV, Protesescu L, Bodnarchuk MI. Properties and potential optoelectronic applications of lead halide perovskite nanocrystals. Science. 2017;**358**:745-750

[7] Gonzalez-Carrero S, Galian RE, Pérez-Prieto J. Maximizing the emissive properties of CH3NH3PbBr3 perovskite nanoparticles. Journal of Materials Chemistry A. 2015;**3**:9187-9193

[8] Moyen E et al. Ligand removal and photo-activation of CsPbBr3 quantum dots for enhanced optoelectronic devices. Nanoscale. 2018;**10**:8591-8599

[9] Hong K, Van Le Q, Kim SY, Jang HW. Low-dimensional halide perovskites: Review and issues. Journal of Materials Chemistry C. 2018;**6**:2189-2209

[10] Wei Y, Cheng Z, Lin J. An overview on enhancing the stability of lead halide perovskite quantum dots and their applications in phosphor-converted LEDs. Chemical Society Reviews. 2019;**48**:310-350

[11] Bella F et al. Improving efficiency and stability of perovskite solar cells with photocurable fluoropolymers. Science. 2016;**354**:203-206

[12] Wang R et al. A review of perovskites solar cell stability. Advanced Functional Materials. 2019;**1808843**:1-25

[13] Song T-B, Yokoyama T, Aramaki S, Kanatzidis MG. Performance enhancement of lead-free tin-based perovskite solar cells with reducing atmosphere-assisted dispersible additive. ACS Energy Letters. 2017;**2**:897-903

[14] Lyu M, Yun J-H, Chen P, Hao M, Wang L. Addressing toxicity of lead: Progress and applications of low-toxic metal halide perovskites and their derivatives. Advanced Energy Materials. 2017;**7**:1602512

[15] Babayigit A et al. Assessing the toxicity of Pb- and Sn-based perovskite solar cells in model organism danio rerio. Scientific Reports. 2016;**6**:18721

[16] Mitzi DB. $N_4H_9Cu_7S_4$: A hydrazinium-based salt with a layered Cu7S4-framework. Inorganic Chemistry. 2007;**46**(3):926-931

[17] Singh RK et al. Exploring the impact of the Pb^{2+} substitution by Cd^{2+} on the structural and morphological properties of $CH_3NH_3PbI_3$ perovskite. Applied Nanoscience. 2019:1-10. https://doi.org/10.1007/s13204-019-01021-5

[18] Kim HS et al. Lead iodide perovskite sensitized all-solid-state submicron thin film mesoscopic solar cell with efficiency exceeding 9%. Scientific Reports. 2012;**2**:591

[19] Singh RK et al. Novel synthesis process of methyl ammonium bromide and effect of particle size on structural, optical and thermodynamic behavior of $CH_3NH_3PbBr_3$ organometallic perovskite light harvester. Journal of Alloys and Compounds. 2018;**743**:728-736

[20] Chen Q et al. Under the spotlight: The organic–inorganic hybrid halide perovskite for optoelectronic applications. Nano Today. 2015;**10**:355-396

[21] Peña MA, Fierro JLG. Chemical structures and performance of perovskite oxides. Chemical Reviews. 2001;**101**:1981-2017

[22] Zhang F et al. Colloidal synthesis of air-stable CH3NH3PbI3 quantum dots by gaining chemical insight into the solvent effects. Chemistry of Materials. 2017;**29**:3793-3799

[23] Zhang S et al. Efficient red perovskite light-emitting diodes based on solution-processed multiple quantum wells. Advanced Materials. 2017;**29**:1606600

[24] Singh RK et al. Solution processed hybrid organic-inorganic CH3NH3PbI3 perovskite material and optical properties. Materials Today: Proceedings. 2017;**4**:12661-12665

[25] Price MB et al. Hot-carrier cooling and photoinduced refractive index changes in organic–inorganic lead halide perovskites. Nature Communications. 2015;**6**:8420

[26] Sheng R et al. Photoluminescence characterisations of a dynamic aging process of organic–inorganic CH3NH3PbBr3 perovskite. Nanoscale. 2016;**8**:1926-1931

[27] Tan Z-K et al. Bright light-emitting diodes based on organometal halide perovskite. Nature Nanotechnology. 2014;**9**:687

[28] Shamsi J, Urban AS, Imran M, De Trizio L, Manna L. Metal halide perovskite nanocrystals: Synthesis, post-synthesis modifications, and their optical properties. Chemical Reviews. 2019;**119**:3296-3348

[29] Hoefler SF, Trimmel G, Rath T. Progress on lead-free metal halide perovskites for photovoltaic applications: A review. Monatshefte für Chemie—Chemical Monthly. 2017;**148**:795-826

[30] Konstantakou M, Stergiopoulos T. A critical review on tin halide perovskite solar cells. Journal of Materials Chemistry A. 2017;**5**:11518-11549

[31] Shum K et al. Synthesis and characterization of CsSnI3 thin films. Applied Physics Letters. 2010;**96**:221903

[32] Chung I et al. CsSnI3: Semiconductor or metal? High electrical conductivity and strong near-infrared photoluminescence from a single material. High hole mobility and phase-transitions. Journal of the American Chemical Society. 2012;**134**:8579-8587

[33] Hou S, Guo Y, Tang Y, Quan Q. Synthesis and stabilization of colloidal perovskite nanocrystals by multidentate polymer micelles. ACS Applied Materials & Interfaces. 2017;**9**:18417-18422

[34] Fang G et al. Reverse synthesis of $CsPb_xMn_{1-x}(Cl/Br)3$ perovskite quantum dots from CsMnCl3 precursors through cation exchange. Journal of Materials Chemistry C. 2018;**6**:5908-5915

[35] Marshall KP, Walker M, Walton RI, Hatton RA. Enhanced stability and efficiency in hole-transport-layer-free CsSnI3 perovskite photovoltaics. Nature Energy. 2016;**1**:16178

[36] Liu F et al. Colloidal synthesis of air-stable alloyed $CsSn_{1-x}Pb_xI_3$ perovskite nanocrystals for use in solar cells. Journal of the American Chemical Society. 2017;**139**:16708-16719

[37] Wang A et al. Controlled synthesis of lead-free and stable perovskite derivative Cs_2SnI_6 nanocrystals via a facile hot-injection process. Chemistry of Materials. 2016;**28**:8132-8140

[38] Eames C et al. Ionic transport in hybrid lead iodide perovskite solar cells. Nature Communications. 2015;**6**:7497

[39] Wang H-C et al. High-performance $CsPb_{1-x}Sn_xBr_3$ perovskite quantum dots for light-emitting diodes. Angewandte Chemie, International Edition. 2017;**56**:13650-13654

[40] Akkerman QA et al. Tuning the optical properties of cesium lead halide perovskite nanocrystals by anion exchange reactions. Journal of the American Chemical Society. 2015;**137**:10276-10281

[41] Buonsanti R, Milliron DJ. Chemistry of doped colloidal nanocrystals. Chemistry of Materials. 2013;**25**:1305-1317

[42] Zhao J. Enhanced luminescence and energy transfer in Mn2+ dopedB-site doped $CsPbCl_3$-xBrx perovskite nanocrystals. Nanoscale. 2018;**10**:19435-19442

[43] Guria AK, Dutta SK, Das Adhikari S, Pradhan N. Doping Mn^{2+} in lead halide perovskite nanocrystals: Successes and challenges. ACS Energy Letters. 2017;**2**:1014-1021

[44] Liu F et al. Highly luminescent phase-stable CsPbI3 perovskite quantum dots achieving near 100% absolute photoluminescence quantum yield. ACS Nano. 2017;**11**:10373-10383

[45] Liu W et al. Mn^{2+}-doped lead halide perovskite nanocrystals with dual-color emission controlled by halide content. Journal of the American Chemical Society. 2016;**138**:14954-14961

[46] Yuan X et al. Photoluminescence temperature dependence, dynamics, and quantum efficiencies in Mn^{2+}-doped $CsPbCl_3$ perovskite nanocrystals with varied dopant concentration. Chemistry of Materials. 2017;**29**:8003-8011

[47] Zhu J et al. Room-temperature synthesis of Mn-doped cesium lead halide quantum dots with high Mn substitution ratio. Journal of Physical Chemistry Letters. 2017;**8**:4167-4171

[48] Zou S et al. Stabilizing cesium lead halide perovskite lattice through Mn(II) substitution for air-stable light-emitting diodes. Journal of the American Chemical Society. 2017;**139**:11443-11450

[49] Akkerman QA, Meggiolaro D, Dang Z, De Angelis F, Manna L. Fluorescent alloy $CsPb_xMn_{1-x}I3$ perovskite nanocrystals with high structural and optical stability. ACS Energy Letters. 2017;**2**:2183-2186

[50] van der Stam W et al. Highly emissive divalent-ion-doped colloidal $CsPb_{1-x}M_xBr_3$ perovskite nanocrystals through cation exchange. Journal of the American Chemical Society. 2017;**139**:4087-4097

[51] Mondal N, De A, Samanta A. Achieving near-unity photoluminescence efficiency for blue-violet-emitting perovskite nanocrystals. ACS Energy Letters. 2019;**4**:32-39